Research Journal of Chemical Sciences _____ ISSN 2231-606X
Vol. **2(1),** 32-37, Jan. **(2012)** *Res.J.Chem.Sci.*

Synthesis and phenol degradation activity of Zn and Cr doped TiO_2 Nanoparticles

Pawar M.J., Nimbalkar V.B.
Laboratory of Materials Synthesis, Department of Chemistry, ACS College, Amravati, INDIA

Available online at: www.isca.in
(Received 12th October 2011, revised 8th November 2011, accepted 15th December 2011)

Abstract

Zn and Cr doped TiO_2 nanoparticles have been prepared by combustion method and characterized by surface analytical methods such as X-ray diffraction (XRD) and Brunauer-Emmett-Teller (BET) nitrogen-gas adsorption method. The band gap energy of Zn and Cr doped TiO_2 obtained by UV-DRS was 2.7 and 2.3 eV, respectively. The photocatalytic activity of catalyst was tested by photocatalytic degradation of phenol. Results show doped TiO_2 is more efficient than pure TiO_2 at photocatalytic degradation of phenol. $Ti_{0.9}Cr_{0.1}O_2$ showed enhanced activity. This enhanced activity was attributed to smaller crystallite size (12.6 nm), synergistic effect between anatase and rutile phases and larger specific surface area (160.11m^2/g).

Keywords: Doped TiO_2 nanoparticles, combustion synthesis, photodegradation of phenol.

Introduction

In recent years, contamination of water by phenol is a serious and widespread issue. Phenol is also a priority pollutant and is included in the list of Environmental Protection Agency (EPA) since 1979. The origin of phenol in the environment is both industrial and natural. Phenol pollution is associated with pulp mills, coal mines, refineries, wood preservation plants and various chemical industries as well as their wastewaters[1]. Natural sources of phenol include forest fire, natural run off from urban area where asphalt is used as the binding material and natural decay of lignocellulosic material. The presence of phenol in water can cause toxic effects on aquatic flora and fauna[2]. Phenols are toxic to human beings and affect several biochemical functions[3].

Many technologies have been investigated for removal and degradation of phenolic compounds in wastewater. They included, adsorption[4], biodegradation[5], UV/Fe (III)[6], extraction by liquid membrane[7], oxidation[8-10]. Apart from these technologies, the photodegradation technology has shown their potential to destroy phenol completely in wastewater. Photodegradation of phenol in presence of UV light using semiconductor metal oxides (such as ZnO, SnO_2, Fe_2O_3, CdO, TiO_2 etc) is an efficient technique in wastewater treatment. Among semiconductor metal oxides, TiO_2 has been the focus of photocatalysis under UV irradiation due to its superiority in the oxidation capacity, non-toxicity, and long-term stability[11]. The surface as well as intrinsic properties of TiO_2 plays an important role in influencing the course of a photochemical reaction. Various doping methods have been extensively utilized for modifying the electronic structures of TiO_2 nanoparticles to achieve new or improved catalytic activities and the other chemical and physical properties. There have been many reports on transition metal[12, 13], noble metal[14, 15] and rare earth[16-20] doping of TiO_2.

In this work, we focus on the investigation of the effect of Zn^{2+} (divalent) and Cr^{3+} (trivalent) ions doping on the phenol degradation activity of TiO_2. $Ti_{1-x}M_xO_2$ (M = Zn^{2+} and Cr^{3+}) nanoparticles were synthesized by combustion method. Combustion synthesis is rapidly emerging as one of the most-convenient methods for the preparation of oxide materials. The main advantage of using this technique is due to the simplicity, the broad applicability range, the self-purifying feature due to the high temperatures involved, the possibility of obtaining products in the desired size and shape. The powders of pure TiO_2, $Ti_{1-x}Zn_xO_2$ and $Ti_{1-x}Cr_xO_2$ were synthesized and effect of calcination temperature and pH of phenolic solution on photocatalytic activity of TiO_2 was discussed.

Material and Methods

Synthesis of photocatalyst: Pure as well as $Ti_{1-x}M_xO_2$ (x = 0.05 0.1; M = Zn and Cr) nanoparticles were synthesized via a combustion method. Briefly, doped TiO_2 nanoparticles were synthesized from titanium iso-propoxide (Ti $(OC_2H_5)_4$) zinc nitrate (Zn $(NO_3)_3$) and cerium nitrate (Ce $(NO_3)_3$) were used as metal sources. The appropriate amount of titanium iso-propoxide was added to the equimolar mixture of citric acid (CA) ethylene glycol (EG) and glucose. The molar ratios of CA/Ti and CA/EG were kept constant at 2:1 and 1:1, respectively. The mixture was kept on hot plate and stirred at 60°C for 1 h. While stirring, the salts of dopants were added to this solution and the stirring was continued for the next 1 h. The amounts of dopants viz. Zn^{2+} and Cr^{3+} are 0.25 mol%. The dopant stoichiometry was controlled prior to

the mixing to titanium salt solution. The pH of solution was maintained in the range 6-7. Stirred solution was further heated at 85°C to get the mixture in gel form. So obtained gel was further baked at 120°C followed by the combustion at 270°C in muffle furnace. The porous powders obtained on combustion in the furnace operating between 500°C in ambient atmosphere for 3 h. The calcined samples were pulverized to fine powders using agate mortar and codification of powders was done and details are presented in Table-1.

Characterization of photocatalyst: The crystalline phase and particle size of TiO_2 nanoparticles (doped and undoped) were analyzed by X-ray diffraction (XRD) measurements which were carried out at room temperature by using Siemens X-ray diffraction D5000 with Cu *K*α radiation (λ = 0.15478 nm). The particle lattice parameters were obtained by the Bragg law (Eq. 1). Besides, the effect of the dopants on the rutile and anatase concentrations in TiO_2 structure was determined from XRD analysis. The mass fraction of rutile (X_r) in the samples was calculated, based on the relationship between the integrated intensities of anatase (101) and rutile (110) peaks using equation: $X_r = 1/(1 + K(I_a/I_r))$ (1)

where, I_a and I_r are the integrated peak intensities of the anatase (101) and rutile (110) peaks, respectively. The constant K (0.79) was determined by XRD analysis of Degussa P-25 of known proportions of anatase and rutile (80:20). Particle size calculations were carried out using Scherrer's equation: $t = 0.9\lambda/\beta\cos\theta$ (2)

where, λ is a wavelength of the radiation, β is full width at half maxima (FWHM) and θ is the diffraction angle. The SEM image of doped and undoped TiO_2 were recorded with SEM LEO 440 i. The values of specific surface areas (S_{BET}) of the calcined powders were measured by Brunauer-Emmett-Teller (BET) nitrogen-gas adsorption method.

Photocatalytic activities: The photocatalytic activity of phenol was studied from photodegradation of phenol from its 0.005 M solution in distilled water. The concentration of phenolic solution was confirmed by spectrophotometer 500 nm. The pH value of the solution was adjusted using the solutions of ammonium hydroxide (0.1 M) and hydrochloric acid (0.1 M). Phenol degradation experiments were conducted in the photochemical cell consisted of pyrex-glass beakers with 250 cm^3 capacity. During the photocatalytic reaction, the solution was irradiated using a 250 W UV light (λ=365 nm). Temperature of cell was maintained at 25°C. A high-pressure mercury lamp was placed in a 50 mm diameter quartz tube. Each beaker was filled with 200 cm^3 of 0.005 M phenol solution. To this solution, 0, 0.050 and 0.100 g/dm^3 pure and doped TiO_2 nanoparticles were added as a catalyst. Before the light is turned on, the solution was stirred for 15 min to ensure good adsorption equilibrium between the catalyst and the solution. During the photocatalytic reaction, the solution was aerated by bubbling air. The magnetic stirrer was employed to keep the solution uniform. Solutions were radiated by UV–vis light for specific time intervals. Experiments were performed for 120 min. At the irradiation time intervals of 15 min., the samples of phenol solution were drawn and analyzed to determine the concentration of phenol.

Results and Discussion

The crystallite sizes of the prepared samples were calculated from both XRD data using Scherrer's formula and BET analysis. Table-1 shows the values of undoped and doped TiO_2 particle sizes. The average particle size ranges between 12 to 36 nm. The crystal structures and average size were confirmed. Besides the range scans (2θ = 20°–50°), high resolution scans for anatase (101) and (200) peaks were carried out with scan speed of 0.05° min and short point interval of 0.002°.

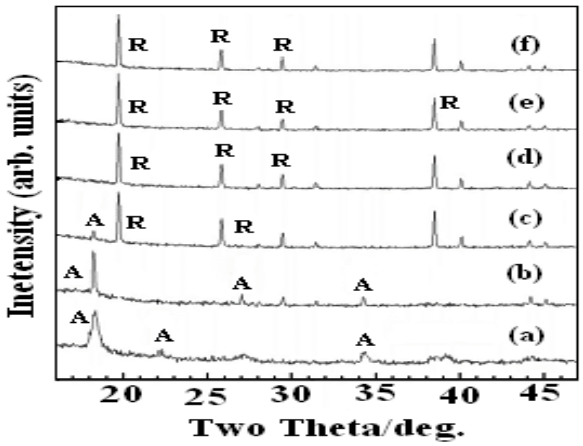

Figure-1a
XRD patterns of pure TiO_2 calcined at temperatures a) 500°C, b) 550°C, c) 600°C, d) 650°C, e) 700°C

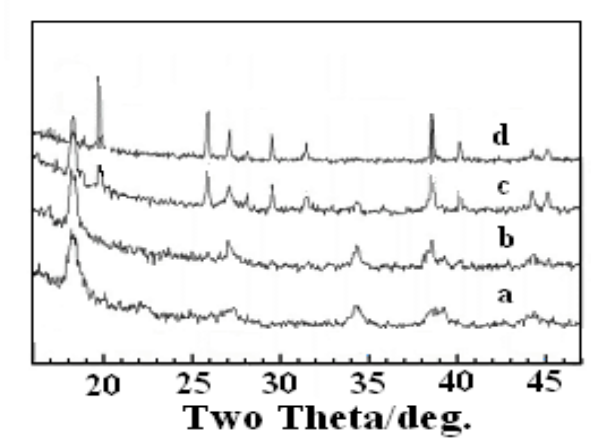

Figure-1b
XRD patterns of a) $Ti_{0.95}Zn_{0.05}O_2$, b) $Ti_{0.9}Zn_{0.1}O_2$, c) $Ti_{0.95}Cr_{0.05}O_2$ and d) $Ti_{0.9}Cr_{0.1}O_2$ calcined at temperature 550°C

XRD pattern of pure TiO_2 powders are shown in Figure-1a. At 500°C, the anatase phase is prominent in as synthesized pure TiO_2 structure. On the other hand, along with anatase phase, rutile phase was also detected by XRD at 550°C. One can see that, as the calcination temperature increases from 600°C to 700°C, rate of anatase to rutile transformation also increases. A complete transformation of anatase TiO_2 into rutile TiO_2 occurs at 700°C. The average particle size for pure TiO_2 samples used in the study was found to be about 45 nm. XRD pattern of doped TiO_2 powders calcined at 550°C are shown in Figure-1b. Zn doped catalyst showed the presence of only anatase phase though its concentration is increased to 0.1 %. It is well known that the anatase phase is thermodynamically stable for smaller crystallites[21]. This suggests that Zn stabilized anatase phase irrespective of their nature, oxidation state and electronic configuration. Moreover, introduction of Zn as dopant also decreases the crystallite size of TiO_2 to 18.9 nm. On the other hand, Cr doped catalyst shows the presence of anatase as well as rutile phases even at 550°C. The transformation anatase phase to rutile phase is accompanied by a crystallographic re-arrangement in TiO_2 lattice which in turn affect its photocatalytic activity. Broad XRD peaks indicate formation of nanosized particles of TiO_2 and their average particle size have been estimated ~12 nm by using Debye–Scheerer equation. No separate dopant related phases were found suggesting little or no dopant oxide phase within the XRD detection limit. This indicates that the doping process did not induce the formation of separate impurity phases and that the specific dopant could be considered to be fully incorporated into TiO_2 lattice. Also, Cr^{3+} ions may be easily substituted into Ti site of TiO_2 because the ionic radius of Cr^{3+} (61.5 pm) is similar to that of Ti^{4+} (60.5 pm).

BET surface areas of the as synthesized samples ranged from 63 to161.4 m^2/g. Powders with smaller particle size had higher surface are. Highest surface area was measured for sample TC-10 with crystallite size 12.6 nm. The surface area of Zn doped samples (TZ-05 and TZ-10) was recorded between 153-162 m^2/g.

The optical properties of various the samples PT-60, TZ-10 and TC-10 were probed by UV-DRS as shown in Figure-2. The main absorption edge of TiO_2 was estimated to at about 388 nm which corresponds to band gap of 3.2 eV. UV absorption spectral studies indicated the band gap extension of the doped samples to visible region. This is due to the creation of impurity levels by the dopant within the band gap states of TiO_2. The samples TZ-10 and TC-10 showed a shoulder peak at a wavelength of around 600 – 450 nm, which was not observed in the spectrum of sample PT-60. The shoulder peaks in the spectrum of doped TiO_2 are probably due to the absorption by the doped metal and oxygen vacancies created by substitution of Ti^{4+}. The energy band gaps estimated from the UV-vis spectra of Zn and Cr doped TiO_2 were 2.7 and 2.3 respectively. The photocatalytic activity of catalysts was evaluated by the degradation of phenol solution (0.005M). The degradation rate was calculated based on an irradiation of the catalyst added phenol solution for 2 h. The change in the photocatalytic activity of TiO_2 by doping Zn^{2+} and Cr^{3+} ions is shown in Figure-3. One can see that, $Ti_{0.9}Cr_{0.1}O_2$ (sample TC-10) is a good photocatalyst for phenol degradation. Zn doped TiO_2 is also a good catalyst for phenol degradation compared to undoped TiO_2. The phenol degradation in 6 min with catalysts PT-60, TZ-05 and TZ-10 was about 34%, 37% and 45% respectively. On the other hand, catalyst TC-05 showed 56% phenol degradation in the same irradiation time. It is clear from the results that doping of Zn^{2+} and Cr^{3+} significantly changes the photocatalytic activity of TiO_2 towards the phenol degradation. The optimum degradation was observed for sample TC-10. The increase in photocatalytic activity on doping is probably due to prevention of electron–hole recombination and the existence of a synergistic effect between anatase and rutile. The highest enhancement in photoreactivity was obtained $Ti_{0.9}Cr_{0.1}O_2$ which may be in favor of the most efficient separation of the charge carriers.

Table-1
Synthetic condition, phase composition, phase content, average crystallite size and specific surface area

Photocatalyst	Code	Calcination temperature (°C)	Phases	Phase composition (%)	Average crystallite size (D_{XRD}) nm	Average crystallite size (D_{BET}) nm	Specific surface area (m^2/g)
TiO_2	PT-50	500	A	100	45.9	36.9	63.45
TiO_2	PT-55	550	R/A	12/88	43.2	35.5	97.2
TiO_2	PT-60	600	R/A	79/21	25.2	29.9	133.47
TiO_2	PT-65	650	R/A	67/37	26.1	33.6	129.33
TiO_2	PT-70	700	R	100	35.1	36.1	88.20
$Ti_{0.95}Zn_{0.05}O_2$	TZ-05	550	A	100	20.7	21.6	146.5
$Ti_{0.90}Zn_{0.10}O_2$	TZ-10	550	A	100	18.9	14.4	150.52
$Ti_{0.95}Cr_{0.05}O_2$	TC-05	550	A/R	75/72	13.5	12.6	160.11
$Ti_{0.90}Cr_{0.10}O_2$	TC-10	550	A/R	/29	12.3	19.8	161.45

Several factors can have a positive impact on the photocatalytic activity doped TiO_2. The particle size and surface area of catalyst were the two important parameters influencing the photocatalytic activity of nanocrystalline TiO_2 (table-1). The particle size of doped TiO_2 samples decreases with the concentration of Zn and Cr. Reduction in crystallite size leads to larger surface area which increases the available surface active sites consequently resulting in higher photonic efficiency. Among all the synthesized samples, particle size of sample TC-10 is smallest (12.3 nm) with surface area 150.21 m^2/g. It was reported that, 10 nm is the optimum particle size of TiO_2 to obtain maximum photocatalytic oxidation rates of organic compounds[21]. However, in our case, the optimum photocatalytic activity was observed for sample TC-10 though its particle size is slightly larger than the optimum value.

The experimental results of the work showed that, the TiO_2 catalyst with dopant concentration x = 0.1 has better photocatalytic activity as compared to catalyst with x = 0.05. This is because the dopants concentration plays an important role in enhancement of photocatalytic activity of TiO_2. As the concentration of dopant ions increases, the surface barrier becomes higher and the electron-hole pairs within the region are efficiently separated. The main objective of doping is to decrease of the band gap or introduction of intra-band gap states, which results in more visible light absorption. In doping, metal ion with smaller ionic radius can penetrate deeply into TiO_2 lattice which can cause a lattice deformation and produce defects in the crystal[23] by substitution of Ti^{4+}. The defects can inhibit the recombination of the electron-hole pairs and, eventually, enhance the activity. The ionic radius of Cr^{3+} ion is smaller (61.5 pm) than that of Zn^{2+} (74 pm) which results in enhanced photocatalytic activity of nanocrystalline TiO_2.

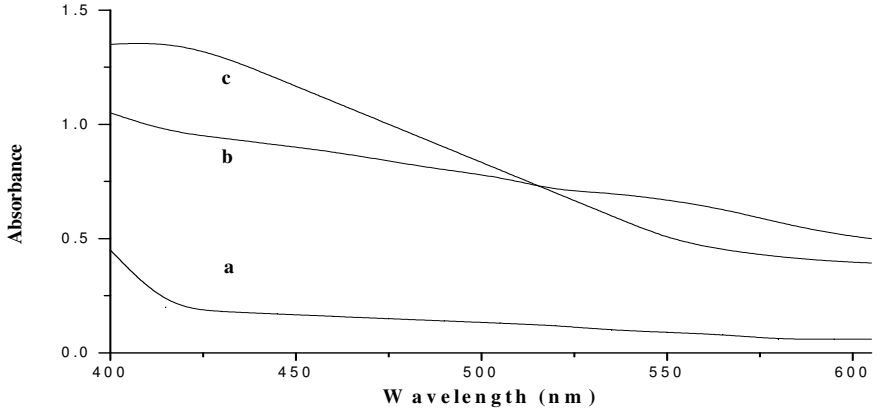

Figure-2
UV-vis diffuse reflectance spectra for samples a) PT-60, b) TZ-10 and c) TC-10

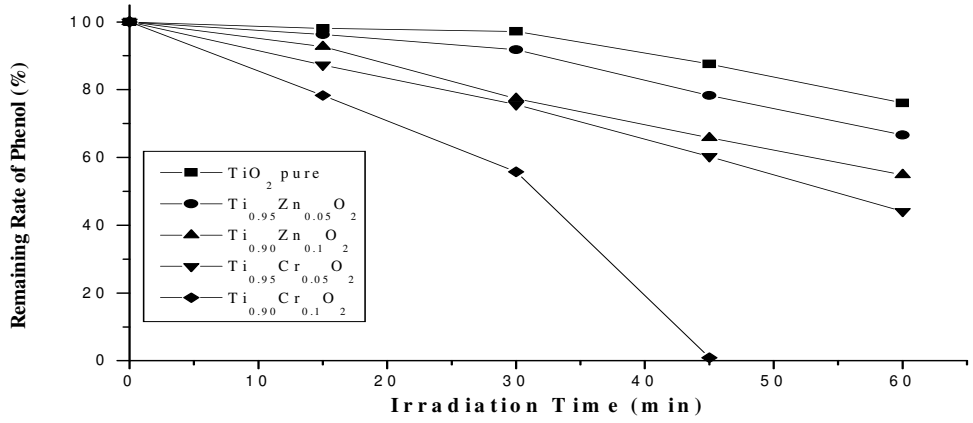

Figure-3
Influence of Zn and Cr doping concentrations on photocatalytic activity of TiO_2 for phenol degradation

Our experiments confirmed the synergetic effect was one of the causes behind the high photocatalytic activity of sample TC-10 for phenol degradation. As the results from XRD studies showed Zn doped TiO_2 samples consist only anatase phases. On the other hand, rutilation starts with Cr doping even at low concentration x = 0.05. The photocatalytic activity of such mixtures mainly depends upon the amounts of anatase and rutile phases. TiO_2 with anatase/rutile ratio of 70/30 showed highest activity for p-coumaric acid degradation [23]. The highest phenol degradation activity of TC-10 could be due to its anatase/rutile ratio (71/29) which is much closer to the ratio reported by earlier researchers[23]. The smaller band gap of rutile phase captures the photons generating electron/hole pairs. The anatase phase traps the electron transferred from the conduction band of rutile phase. This mechanism inhibits the recombination of electron as well as holes and the photocatalytic activity is improved.

Conclusions

Pure and Zn and Cr doped TiO_2 nanoparticles have been synthesized by combustion method. The photocatalytic activities of the catalysts were tested under UV light for the degradation of phenol as a probe molecule. XRD results confirmed that Zn doping significantly inhibit the anatase-to-rutile phase transformation and rutilation was promoted with Cr doping. Present study shows improvement of TiO_2 photocatalytic activity upon Zn and Cr doping compared to pure TiO_2. The difference in photocatalytic activity of pure TiO_2 and doped TiO_2 can be attributed to the characteristic such as particle size and anatase/rutile ratio.

The highest enhancement in photoreactivity was obtained for $Ti_{0.9}Cr_{0.1}O_2$ nanoparticles consists of mixed phases with 25% rutile shows the highest photocatalytic activity, which suggests the existence of a synergistic effect between anatase and rutile phases. Moreover, the fine particle size and large specific surface area of $Ti_{0.9}Cr_{0.1}O_2$ are the other probable causes for high photocatalytic activity of the catalyst.

References

1. Paula M., Van Schei and Young L.Y., Isolation and Characterization of phenol degrading denitrifying bacteria, *Applied and Environmental Microbiology*, **64,** 2432-2438 (**1998**)

2. Ghadhi S.C. and Sangodkar UMX, Potentials of Pseudomonas cepacia PAA in bioremediation of aquatic wastes containing phenol, Proceedings of National symposium frontiers in applied and environmental microbiology, Cochin 11-13 (December **1995**)

3. Nuhoglu A. and Yakin B., *Modeling of phenol removal in a batch reactor,* Process of Biochemistry, **40**, 233-239 (**2005**)

4. Rengaraj S., Moon S.H., Sivablan R., Arabind B. and Murugesan V., Removal of phenol from aqueous solution and resin manufacturing industry wastewater using an agricultural waste: rubber seed coat, *Journal of Hazardous Materials,* **89,** 185-196 (**2002**)

5. Miland E., Smyth M.R. and Fagain C.O., Phenol removal by modified peroxidases, *Journal of Chemical Technology and Biotechnology,* **67,** 227-236 (**1996**)

6. Zhou M., Wu Z. and Dahui W. Promoted UV/Fe^{+3} process for p-nitropheol degradation by electrocatalysis, In: Proceedings of The International Water Association Conference on Water and Wastewater Management for Developing Countries, PWTC, Kuala Lumpur, Malaysia, **1**, 222-237 (**October 2001**)

7. Lin S.H., Pan C.L. and Leu H.G. Liquid membrane extraction of 2-chlorophenol from aqueous solutions, *Journal of Hazardous Materials,* **65,** 289-304 (**1999**)

8. Benitez F.J., Beltran-Heredia J., Acero J.L. and Rubio F.J., Oxidation of several chorophenolic derivatives by UV irradiation and hydroxyl radicals, *Journal of Chemical Technology and Biotechnology,* **76,** 312-320 (**2001**)

9. Comninellis C. and Pulgarin C., Anoxic oxidation of phenol for wastewater treatment, *Journal of Applied Electrochemistry,* **21,** 703-708 (**1991**)

10. Tahar N.B. and Savall A., Mechanistic aspects of phenol electrochemical degradation by oxidation on a Ta/PbO_2 anode, *Journal of Electrochemical Society,* **145,** 3427-3434 (**1998**)

11. Fujihira M., Satoh Y., Osa T., Heterogeneous photocatalytic oxidation of aromatic compounds on TiO_2, *Nature,* **293,** 206–208 (**1981**)

12. Choi W., Termin A. and Hoffmann M.R., The role of Metal ion dopants in quantum sized TiO2; correlation between photoreactivity and charge carrier recombination dynamics, *J. Phys. Chem*., **98,** 13669–13679 **(1994)**

13. Kim D.H., Woo S.I., Moon S.H., Kim H.D., Kim B.Y., Cho J.H., Joh Y.G. and Kim E.C., Effect of Co/Fe co-doping in TiO2 rutile prepared by solid state reaction, *Solid State Commun*., **136,** 554–558 **(2005)**

14. Chen H., Chen S., Quan X., Yu H.T., Zhao H.M. and Zhang Y.B., Fabrication of TiO_2-Pt coaxial nanotube array Schottky structures for enhanced photocatalytic degradation of phenol in aqueous solution, *Journal of Phys. Chem. C*., **112,** 9285–9290 **(2008)**

15. Chen J.L, Loso E., Ebrahim N. and Ozin G.A. Synergy of slow photon and chemically amplified photochemistry in platinum nanocluster-loaded

inverse titania opals, *Journal of American Chemical Society.* **130,** 5420–5421 **(2008)**

16. Ranjit K.T., Willner I., Bossmann S.H. and Braun A.M., Lanthanum oxide doped titanium dioxide photocatalysts: Effective catalysts for the enhanced degradation of the salicylic acid and t-cinnamic acid, *J. Catal*., **204,** 305–313 **(2001)**

17. Zhang Y., Xu H., Xu Y., Zhang H. and Wang Y., The effect of lanthanide on the degradation of RB in nanocrystalline Ln/TiO_2 aqueous solution, *J. Photochem. Photobiol. A: Chem.,* **170,** 279–285 **(2005)**

18. Xiaoli Y., He J., Evans D.G., Duan X. and Zhu Y., Effect of TiO_2 thin film thickness and specific surface area by low-pressure metal–organic chemical vapor deposition on photocatalytic activities, *Applied Catalysis B Environmental*., **55,** 243–252 **(2005)**

19. Xie, Y., Yuan, C. and Li, X. Phosensitized and photocatalyzed degradation of azo dye using Ln^{n+}-TiO_2 sol in aqueous solution under visible light, *Material Science Engineering B*., **117,** 325–333 **(2005)**

20. Baiju K.V., Periyat P., Wunderlich W., Pillai P.K., Mukundan P. and Warrier K.G.K., Enhanced photoactivity of neodymium doped mesoporous titania synthesized through aqueous sol–gel method. *Journal of Sol–Gel Science and Technology*. **43,** 283 **(2007)**

21. Zhang Z.B., Wang C.C., Zakaria R. and Ying J.Y. Role of Particle Size in Nanocrystalline TiO_2-Based Photocatalysts, *Journal of Phys Chemistry B*., **102,** 10871-10878 **(1998)**

22. Rodriguez-Talavera R., Vargas S., Arroyo-Murillo R., Montiel-Campos R. and Haro-Poniatowski E. Modification of the phase transition temperatures in titania doped with various cations, *Journal of Materials Research,* **12,** 439-443 **(1997)**

23. Bacsa R.R. and Kiwi J., Effect of rutile phase on photocatalytic properties of nanocrystalline titania during the degradation of p-coumaric acid, *Applied Catalysis B: Environmental*, **16,** 19-29 **(1998)**